

Article

Spatiotemporal Evolution and Prediction of Ecosystem Carbon Storage in the Yiluo River Basin Based on the PLUS-InVEST Model

Lei Li ¹, Guangxing Ji ¹ , Qingsong Li ¹, Jincui Zhang ¹, Huishan Gao ¹, Mengya Jia ², Meng Li ¹ and Genming Li ^{1,*}

¹ College of Resources and Environmental Sciences, Henan Agricultural University, Zhengzhou 450046, China; leili@stu.henau.edu.cn (L.L.); guangxingji@henau.edu.cn (G.J.); lqsdavid@126.com (Q.L.); zhangjincui3711@163.com (J.Z.); huishan@stu.henau.edu.cn (H.G.); limeng@stu.henau.edu.cn (M.L.)

² School of Hydraulic and Environmental Engineering, Changsha University of Science & Technology, Changsha 410114, China; mjia@live.esu.edu

* Correspondence: gm.li@henau.edu.cn

Abstract: Land-use change has a great impact on regional ecosystem balance and carbon storage, so it is of great significance to study future land-use types and carbon storage in a region to optimize the regional land-use structure. Based on the existing land-use data and the different scenarios of the shared socioeconomic pathway and the representative concentration pathway (SSP-RCP) provided by CMIP6, this study used the PLUS model to predict future land use and the InVEST model to predict the carbon storage in the study area in the historical period and under different scenarios in the future. The results show the following: (1) The change in land use will lead to a change in carbon storage. From 2000 to 2020, the conversion of cultivated land to construction land was the main transfer type, which was also an important reason for the decrease in regional carbon storage. (2) Under the three scenarios, the SSP126 scenario has the smallest share of arable land area, while this scenario has the largest share of woodland and grassland land area, and none of the three scenarios shows a significant decrease in woodland area. (3) From 2020 to 2050, the carbon stocks in the study area under the three scenarios, SSP126, SSP245, and SSP585, all show different degrees of decline, decreasing to $36,405.0204 \times 10^4$ t, $36,251.4402 \times 10^4$ t, and $36,190.4066 \times 10^4$ t, respectively. Restricting the conversion of land with a high carbon storage capacity to land with a low carbon storage capacity is conducive to the benign development of regional carbon storage. This study can provide a reference for the adjustment and management of future land-use structures in the region.

Keywords: land-use change; carbon stocks; CMIP6; PLUS model; InVEST model



Citation: Li, L.; Ji, G.; Li, Q.; Zhang, J.; Gao, H.; Jia, M.; Li, M.; Li, G. Spatiotemporal Evolution and Prediction of Ecosystem Carbon Storage in the Yiluo River Basin Based on the PLUS-InVEST Model. *Forests* **2023**, *14*, 2442. <https://doi.org/10.3390/f14122442>

Academic Editor: Tommaso Sitzia

Received: 14 November 2023

Revised: 6 December 2023

Accepted: 11 December 2023

Published: 14 December 2023



Copyright: © 2023 by the authors. Licensee MDPI, Basel, Switzerland. This article is an open access article distributed under the terms and conditions of the Creative Commons Attribution (CC BY) license (<https://creativecommons.org/licenses/by/4.0/>).

1. Introduction

Since the second industrial revolution, a large amount of greenhouse gases, mainly carbon dioxide, have been emitted, resulting in rising global temperatures and frequent extreme weather [1–3]. Since China's reform and opening up, China's economy has developed rapidly, the proportion of construction land has risen rapidly, and China's carbon emissions have reached first place in the world [4]. In the face of common global challenges, General Secretary Xi Jinping made an important speech at the 75th session of the United Nations General Assembly on the carbon peak in 2030 and carbon neutrality in 2060 [5]. The process of the carbon cycle in terrestrial ecosystems is often accompanied by carbon exchange, and land-use change is the main factor affecting regional carbon balance [6]. Studying the intrinsic relationship between carbon storage and land use can provide a reference for regional development and even increase regional carbon storage under the premise of ensuring economic development.

The traditional methods of carbon storage assessment have shortcomings in research scale, temporal and spatial changes in carbon storage, and visual expression. Moreover, the

operation is complex and costly, and it is not suitable for large-scale carbon storage research, such as the biomass method, accumulation method, and field sampling method [7,8]. In recent years, InVEST has attracted the attention of scholars due to its simple parameters, small amount of data required, and high accuracy [9]. The InVEST model is a model developed by Stanford University in the United States, which can be applied to quantify ecosystem services [10]. Many scholars at home and abroad use the carbon storage plate in the InVEST model to predict carbon storage. For example, Tadese and Rajbanshi studied the relationship between land-use change and carbon storage in the Majang Forest Biosphere Reserve and the Konar catchment, India, respectively [11,12]. Xie [13], Wang [14], and Qing [15] estimated carbon storage and predicted different scenarios for the Huaihai Economic Zone, the Hubao and Yuyu urban agglomeration, and the Shihezi River Basin, respectively. Some scholars use land-use simulation models such as Dyna-CLUE, FLUS, CA-Markov, and other land-use simulation models coupled with InVEST models to predict future carbon stocks. Although the above methods can well simulate future land-use changes, they cannot find out the potential driving factors of land-use changes and the evolution of patches [8,16]. On the basis of these shortcomings, Liang [17] and other scholars proposed the PLUS model, which can improve the mining of transformation rules and the lack of landscape dynamic simulation and obtain higher simulation accuracy and more realistic landscape pattern indicators. At present, many scholars have coupled the InVEST and PLUS models to estimate and predict carbon stocks at provincial levels [18–20] and in urban agglomerations [21,22], cities [23,24], and counties [25]. At present, in the scenario provided by CMIP6, there are relatively few studies coupling the InVEST and PLUS models for research on basin. Therefore, this paper takes the Yiluo River Basin as the research object to evaluate the relationship between regional land-use change and carbon stock change.

The Yiluo River, composed of the Yi River and the Luo River, is one of the ten major tributaries of the Yellow River, and the Yellow River Basin is an indispensable ecological barrier in China [26,27]. In this paper, the PLUS model and InVEST model are coupled to simulate the prediction of carbon stocks in the study area for different periods in the future based on different scenarios provided by CMIP6. In this paper, the land-use change regulation between 2010 and 2020 is used to simulate and predict the land-use status of the study area in 2030, 2040, and 2050. Based on The InVEST model, this paper explores the relationship between land-use change and regional carbon storage in the Yiluo River Basin in different periods. It is expected to point out the trend of carbon stock changes in the basin in recent years and provide a reference for the future development of surrounding cities so as to promote the benign development of carbon storage in the basin.

2. Data Sources and Methodology

2.1. Overview of the Study Area

The Yiluo River Basin originates in Luanchuan County at the southern foot of the Xiong'er Mountain, with a total length of 974 km, passing through Shaanxi Province and Henan Province and mainly flowing through Shangluo City, Sanmenxia City, and Luoyang City. Most of them belong to the Henan boundary, of which the Luoyang section accounts for approximately 59.73% of the total area (Figure 1). The Yiluo River Basin covers an area of approximately 18,881 km², located between 109°43'~113°11' E longitude and 33°39'~34°54' N latitude, and it is located in the transition zone of the second and third tiers in China, with various landform types. The overall trend of the region is low in the east and high in the west, high in the north and south, and low in the middle. The region belongs to the warm temperate continental monsoon climate, summer and autumn are hot and rainy, and spring and winter are cold and dry [28]. The region is rich in mineral resources, and a series of enterprises such as mineral mining, processing, and transportation have been formed in the basin, which play a supporting role in local development.

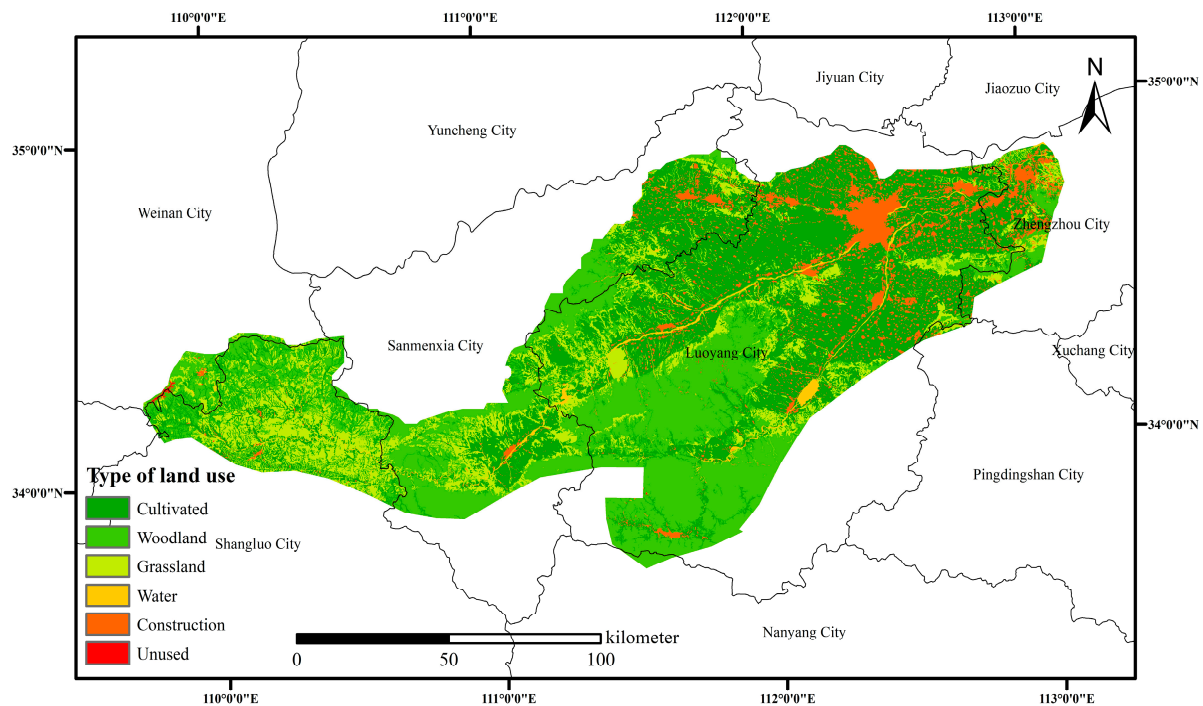


Figure 1. Overview of the Yiluo River Basin.

2.2. Data Sources

The 30 m land-use type, night light, population, GDP, and DEM data required for this study from 2000 to 2020 were obtained from the Resource and Environmental Science and Data Center of the Chinese Academy of Sciences (<https://www.resdc.cn/> (accessed on 18 September 2023)). Road and town data were sourced from OpenStreetMap (<https://www.openhistoricalmap.org/> (accessed on 20 September 2023)). Land-use data from 2030 to 2050 were sourced from the Global 0.25° × 0.25° Land-Use Harmonization (LUH2) dataset (<https://luh.umd.edu/data.shtml> (accessed on 23 September 2023)). Soil-root oxygen content data were sourced from the Harmonized World Soil Database (HWSD) (<http://webarchive.iiasa.ac.at/Research/LUC/External-World-soil-database/> (accessed on 27 September 2023)). On the basis of the original data, ArcGIS was used to process the original data to ensure that the coordinate system was unified (Krasovsky_1940_Albers), the number of rows and columns was unified, and the accuracy of the land-use raster data was unified to 100 m × 100 m (Table 1).

Table 1. Sources of data.

Data Type	Data Name	Data Source
Social factors	Night lights	The Resource and Environmental Science and Data Center of Chinese Academy of Sciences
	Population	The Resource and Environmental Science and Data Center of Chinese Academy of Sciences
	GDP	The Resource and Environmental Science and Data Center of Chinese Academy of Sciences
Locational factors	Railway	OpenStreetMap
	Expressway	OpenStreetMap
	National highway	OpenStreetMap
	Provincial highway	OpenStreetMap
	Town	OpenStreetMap
	City	OpenStreetMap
Natural factors	Land-use data 2000–2020	The Resource and Environmental Science and Data Center of Chinese Academy of Sciences
	Land-use data 2030–2050	The Global 0.25° × 0.25° Land-Use Harmonization (LUH2) dataset
	Soil-root oxygen content	The Harmonized World Soil Database (HWSD)
	Soil types	The Resource and Environmental Science and Data Center of Chinese Academy of Sciences
	DEM	The Resource and Environmental Science and Data Center of Chinese Academy of Sciences
	Slope	Derived from extracting DEM data
	Slope orientation	Derived from extracting DEM data

2.3. Research Method

2.3.1. PLUS Model

The PLUS model is a model that generates land-use change simulations at the patch level and can better explore land-use drivers and sustainable landscape layouts. The PLUS model includes the Land Expansion Analysis Strategy (LEAS) and the CA Model (CARS) based on multi-type random plaque seeds [21,29]. Land expansion analysis strategy rule mining is used to obtain the development probabilities of various types of land use by extracting the parts of various types of land-use expansion in different time slices of land-use change and using the random forest algorithm to excavate the relationship between various types of land-use expansion and driving factors one by one. In the CA module, the expansion probability of each type of land based on the LEAS model was input, and the parameters of land-use conversion rules and domain weights were set to obtain the prediction results. The conversion rules and domain weights used in the CA module were set based on previous studies and the actual situation of the research area [30,31]. The Kappa coefficient was calculated by comparing the predicted land-use type with the real land-use type. If the Kappa coefficient was high, the land-use type under different scenarios in the future could be predicted.

2.3.2. InVEST Model

The InVEST model includes modules for assessing habitat quality, water supply, carbon stocks, and more [32]. In the assessment of carbon stocks, the carbon stocks in the ecosystem are divided into four basic carbon pools: above-ground biochar (C_{above}), below-ground biochar (C_{below}), soil carbon (C_{soil}), and dead organic carbon (C_{soil}). The formula for calculating total carbon stocks is:

$$C_i = C_{i-above} + C_{i-below} + C_{i-soil} + C_{i-dead}$$

$$C_{totali} = \sum_{i=1}^n C_i \times A_i$$

In the formula, i is a certain land-use type; C_i is the carbon density of land use in category i ; and $C_{i-above}$, $C_{i-below}$, C_{i-soil} , and C_{i-dead} are the aboveground vegetation carbon density ($t \cdot hm^{-2}$), belowground vegetation carbon density ($t \cdot hm^{-2}$), soil carbon density ($t \cdot hm^{-2}$), and dead organic carbon density ($t \cdot hm^{-2}$) of type i land-use types, respectively. C_{total} is the total carbon stock of the ecosystem (t), A_i is the area of the type i land-use type (hm^2), and n is the number of land-use types.

The method of determining carbon density data is to use the average annual temperature and average annual precipitation in the study area and the nearby areas, and according to the carbon density correction formula, modify the carbon density of the nearby areas, and then obtain the carbon density of the study area. In this paper, the carbon density of the Yellow River Basin was selected to be corrected, and the average annual temperature and precipitation of the Yiluo River Basin and the Yellow River Basin were 680.1 mm/449.4 mm and 7.05 °C/13.1 °C, respectively [27,33]. The carbon density correction formula is [34–36]:

$$C_{SP} = 3.3968 \times P + 3996.1 \left(R^2 = 0.11 \right)$$

$$C_{BP} = 6.7981e^{0.00541P} \left(R^2 = 0.70 \right)$$

$$C_{BT} = 28 \times T + 398 \left(R^2 = 0.47, P < 0.01 \right)$$

In the formula, C_{sp} is the soil carbon density ($kg \cdot m^{-2}$) obtained based on the average annual precipitation, and C_{bp} and C_{bt} are the biomass carbon density ($kg \cdot m^{-2}$) obtained

based on the average annual precipitation and average annual temperature, respectively. P is the average annual precipitation (mm), and T is the average annual temperature ($^{\circ}\text{C}$).

$$K_{BP} = \frac{C'_{BP}}{C''_{BP}}$$

$$K_{BT} = \frac{C'_{BT}}{C''_{BT}}$$

$$K_B = K_{BT} \times K_{BP}$$

$$K_S = \frac{C'_{SP}}{C''_{SP}}$$

In the formula, K_{BP} and K_{BT} are the correction factors for the precipitation and temperature factors of the biomass carbon density, respectively, and C'_{BP} and C''_{BP} are the biomass carbon density data based on the average annual precipitation in the Yiluo River Basin and the Yellow River Basin, respectively. C'_{BT} and C''_{BT} are the biomass carbon density data of Yiluo River Basin and Yellow River Basin based on average annual temperature, respectively. C'_{SP} and C''_{SP} are the soil carbon density data of the Yiluo River Basin and Yellow River Basin based on average annual temperature, respectively. K_B and K_S are the correction coefficients of the biomass carbon density and the soil carbon density, respectively. According to the calculated carbon density correction coefficient, the carbon density data of the Yellow River Basin were corrected to obtain the carbon density data used in this paper (Table 2).

Table 2. Carbon density data of the study area.

Table	C_{above}	C_{below}	C_{soil}	C_{dead}
Cultivated	22.1	104.9	36.0	12.7
Woodland	55.1	150.7	52.7	18.3
Grassland	45.9	112.5	33.1	9.8
Water	0.4	0.0	0.0	0.0
Construction	3.3	35.8	0.0	0.0
Unused	1.7	0.0	7.2	0.0

3. Results and Analysis

3.1. Land-Use Change from 2000 to 2020

The construction land of the Yiluo River Basin is mainly concentrated in the northeast of the region, that is, the urban area of Luoyang. The cultivated land is mainly distributed in the relatively flat area in the lower reaches of the watershed, which envelops the urban area of Luoyang. Grassland and woodland are mainly concentrated in the middle and upper reaches of the watershed (Figure 2). From 2000 to 2010, 441.82 hectares of cultivated land was transferred to construction land in the Yiluo River Basin, accounting for 83.89% of the total amount of cultivated land transferred. The area of forest land and grassland decreased, mainly due to the conversion to cultivated land, which was 38.52 hectares and 69.06 hectares, respectively, and they accounted for 47.28% and 52.29% of the total transfers, respectively. By 2010, the construction land increased by 351.25 hectares, and the main reason for the increase was the encroachment of construction land on cultivated land. In the decade from 2010 to 2020, the loss of cultivated land mainly went to forest land and construction land, reaching 188.91 hectares and 210.51 hectares, respectively. At this stage, the area of cultivated land converted into construction land was only 47.65% of that in the previous decade. The total areas of forest land and grassland slightly fluctuated, which mainly showed the mutual transformations between cultivated land, forest land, and grassland. The changes in land-use types in the study area were mainly the transfer in and

transfer out of cultivated land and construction land, and most of them occurred within the boundaries of Luoyang. The slowing down of the total conversion degree of various types of land to construction land was related to the entry of a new era and the implementation of water control and revitalization actions in Luoyang City. Luoyang City actively promotes comprehensive water environment management, systematic restoration, and the improvement of water ecology. Luoyang City implemented comprehensive management of the upstream and downstream and left and right banks of the “Four Rivers and Five Canals” in the Yiluo River Basin and carried out the construction of river composite ecological corridors and mountain ecological greening. The forest coverage rate has reached 45.8%, the wetland protection rate has reached 55%, and the soil and water conservation rate has reached 70%. Germplasm resource reserves have been designated, and biodiversity is increasing year by year.

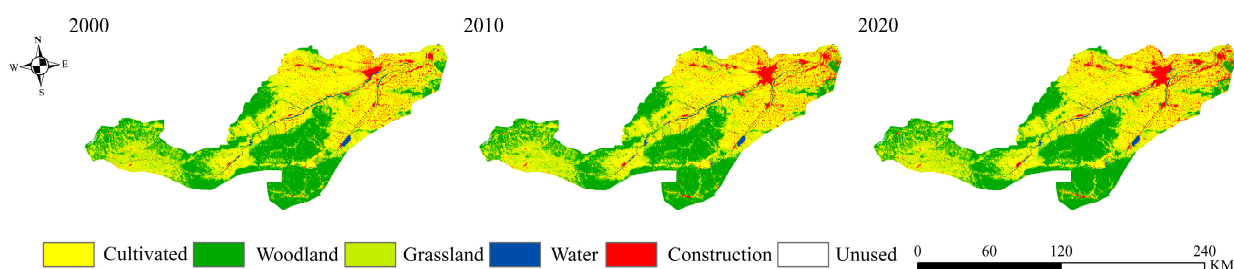


Figure 2. Spatiotemporal evolution of land use from 2000 to 2020.

Overall, cultivated land is the main type of land use in the Yiluo River Basin, and the cultivated land area reached 42.84% of the total area in 2020 (Table 3). The largest area change in the past 20 years has been in cultivated land occupied by construction land, which occupies a total of 593.879 hectares in the past 20 years. The construction land in 2020 was 1.59 times the area in 2000. The increase in the building area is concentrated in the Luoyang section of the Yiluo River Basin, which is related to the rapid economic development in Luoyang in the past 20 years. The other obvious ones are the mutual transformations between arable land, forest land, grassland, and water land. In 2020, in addition to the increase in the area of forest land, the land uses of cultivated land, grassland, and water area all showed different degrees of reduction.

Table 3. Land-use transfer matrix from 2000 to 2020 (km²).

2000	2020						Total
	Cultivated	Woodland	Grassland	Water	Construction	Unused	
Cultivated	7518.743	198.940	132.989	30.293	593.879	0.176	8475.021
Woodland	164.991	5786.434	101.878	8.979	22.598	2.931	6087.812
Grassland	175.317	110.143	2792.163	5.427	48.448	1.419	3132.916
Water	50.240	5.189	6.235	252.246	17.275	0.010	331.194
Construction	178.962	2.444	1.916	1.647	654.486	0.062	839.517
Unused	0.352	2.610	0.145		0.663	10.771	14.541
Total	8088.605	6105.760	3035.325	298.591	1337.349	15.369	18,881.000

3.2. Multi-Scenario Land-Use Change Simulation Based on PLUS Model

According to the actual situation of the study area, 13 driving factors were selected from three aspects: social factors (population and GDP), location factors (distance to railway, distance to expressway, distance to national highway, distance to provincial highway, distance to city, and distance to town), and natural factors (DEM, slope, slope direction, soil type, and oxygen content in soil-roots). The driving factor data were input into the LEAS module of the PLUS model to obtain the contribution degrees of different driving factors to various land-use changes and the expansion probabilities of various land types. The

land-use data of 2020 were predicted with the land-use data of 2010 and compared with the actual land-use data of 2020, and the comparison chart was finally obtained (Figure 3). The Kappa coefficient reached 0.896, and the overall accuracy was 0.929. The simulation results were more accurate, which can be used to predict future land use. Afterward, the land-use data for 2030, 2040, and 2050 were projected via the CA module in the PLUS model by combining the land-use data under different SSP-RCP scenarios.

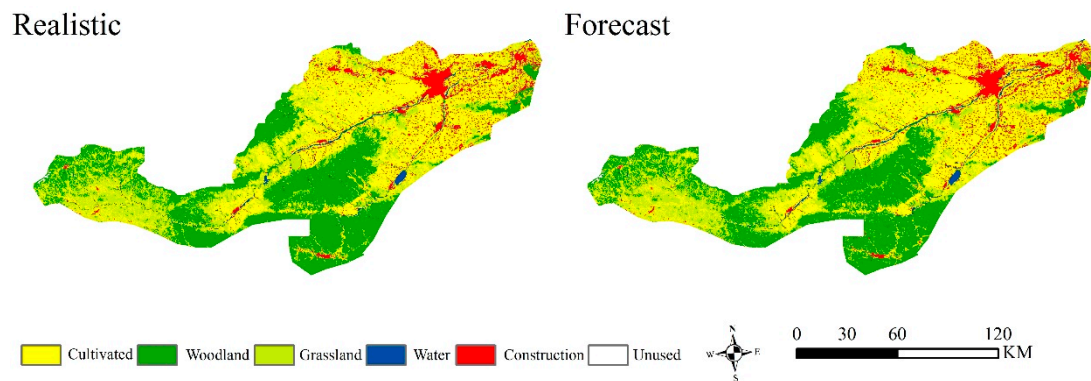


Figure 3. Chart comparison of reality and forecast of land-use types in 2020.

The CMIP emphasizes the impact of different development approaches on future climate change, combining different SSP-RCP scenarios. Five different scenarios are described for the future, depending on the rate at which greenhouse gases are emitted. SSP119 (the scenario combining SSP1 and RCP1.9) is the ideal scenario to reduce global carbon emissions to zero by approximately 2050. SSP126 (coupling SSP1 and RCP2.6) is a more moderate and eco-friendly sustainable development scenario with lower greenhouse gas emissions, with carbon emissions declining at a slower rate and reaching zero after 2050. SSP245 (the scenario that couples SSP2 and RCP4.5) is equivalent to a compromise scenario, representing the middle way for society, with moderate greenhouse gas emissions. Under the SSP370 (the scenario coupling SSP3 and RCP7.0), both carbon emissions and temperatures will rise, and carbon emissions will approximately double by the end of the century. SSP585 (coupling the SSP5 and RCP8.5 scenarios) is a high-speed development scenario dominated by fossil fuels, which is a barbaric development, the pursuit of development at all costs [37,38]. In this paper, three scenarios, SSP126, SSP245, and SSP585, were selected to predict carbon storage in the study area by considering the possibility of future development and the status of the study area [16].

Based on the current changes in land-use types, this paper predicted the land-use types under different scenarios in 2030, 2040, and 2050. In the forecast for the three different time periods, it was shown that under the SSP126 scenario, the cultivated land area will decrease to 8066.58 hectares by 2030, with a total decrease of 22.02 hectares, which is a small decrease. From 2030 to 2050, the cultivated land area shows a fluctuating trend of first increasing and then decreasing. At the end of the period, compared with 2020, the cultivated land area will decrease by 118.38 hectares, with a decrease of only 1.46%. In 30 years, forest land will increase significantly, and by 2050, the total area of this area will increase by 351.88 hectares, an increase of 5.76%. Grassland is decreasing year by year and will decrease by 455.08 hectares in 2050, with a change rate of 14.99%. The area of construction land will increase relatively rapidly before 2040, but there will be no significant change from 2040 to 2050, with a total increase of 220.63 hectares over the preceding 30 years.

Under the SSP245 scenario, the cultivated land area shows a trend of increasing year by year, reaching 8893.85 hectares by 2050, with a total increase of 805.24 hectares during the period, an increase of 9.96%. In this scenario, the change in forest area is relatively small, with a total increase of 75.51 hectares between 2020 and 2030, while the change is not significant in the following 20 years, with a total increase of 82.81 hectares by 2050. Grassland area will decrease rapidly between 2020 and 2050, with a total loss

of 936.98 hectares in 30 years, accounting for 30.87% of the total area. The change trend of construction land area is similar to that under the SSP126 scenario, but the change amplitude is relatively small, with an increase of only 48.14 hectares in 30 years (Table 4).

Table 4. Areas of land-use types under different scenarios for the future period (km²).

Year	SSP126			SSP245			SSP585		
	2030	2040	2050	2030	2040	2050	2030	2040	2050
Cultivated	8066.58	8097.63	7970.22	8337.60	8597.56	8893.85	8591.40	8771.78	8866.43
Woodland	6105.55	6237.27	6457.63	6181.06	6189.20	6188.37	6015.33	6046.18	6085.90
Grassland	2902.83	2674.57	2580.24	2679.77	2395.78	2098.34	2604.28	2380.52	2234.17
Water	298.56	298.56	298.56	298.56	298.56	298.56	298.56	298.56	298.56
Construction	1490.84	1556.50	1557.98	1367.40	1383.41	1385.49	1354.67	1367.23	1379.25
Unused	16.64	16.47	16.36	16.60	16.50	16.40	16.76	16.72	16.69

The largest change in the cultivated area occurs under the SSP585 scenario, while this scenario has the largest change in area between 2020 and 2030, with an increase of 6.22 percent. In the following 20 years, although the cultivated land area still increases, the increase rate is relatively lower, and the total area of cultivated land increases by 777.82 hectares in 30 years, with an increase rate of 9.62%. The area of forest land decreases in the first 10 years and then increases in the next 20 years. By 2050, the total amount of forest land will decrease by 19.86 hectares. The trend of grassland changes from 2020 to 2050 is similar to that of grassland area changes under the SSP245 scenario, but the decrease is relatively small, with a total reduction of 801.15 hectares, a decrease of 26.39%. The area of construction land will change minimally, with a total increase of 41.90 hectares by 2050.

The changes in the areas of water land and unused land in all three scenarios are relatively small. In the three scenarios of the 2050 node, the construction land under the SSP126 scenario is the largest, but at the same time, the forest and grassland areas under the SSP126 scenario are greater than those of the same land type areas under the SSP245 and SSP585 scenarios. The construction land area under the SSP126 scenario is relatively concentrated compared with SSP245 and SSP585. Under the three different scenarios, the increase in construction land mostly occurs around the urban area of Luoyang and the Zhengzhou section of the Yiluo River Basin (Figures 4 and 5).

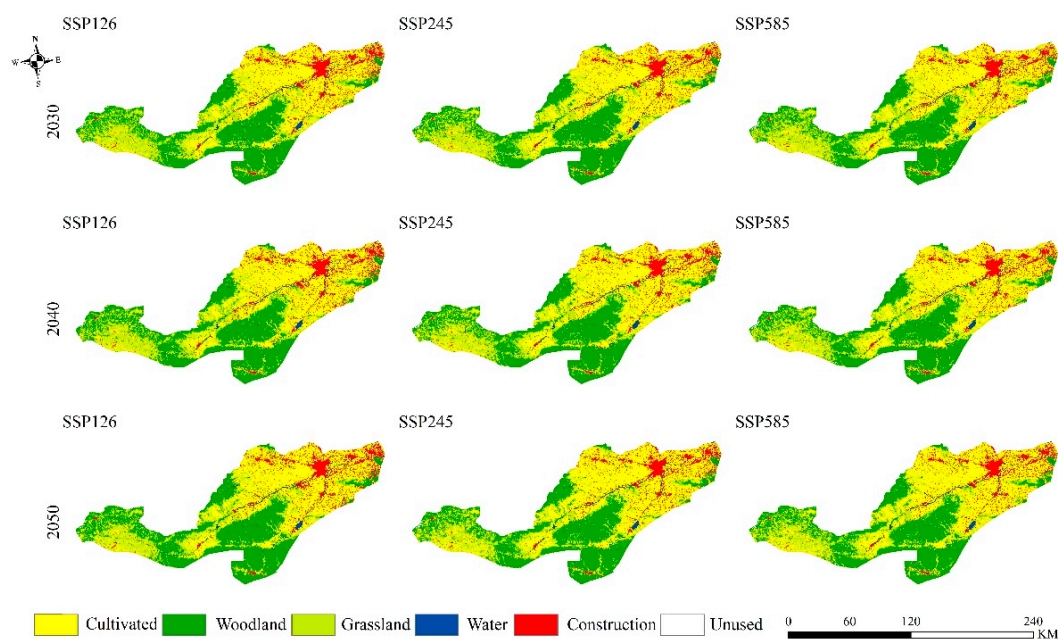


Figure 4. Spatiotemporal evolution of land use from 2030 to 2050.

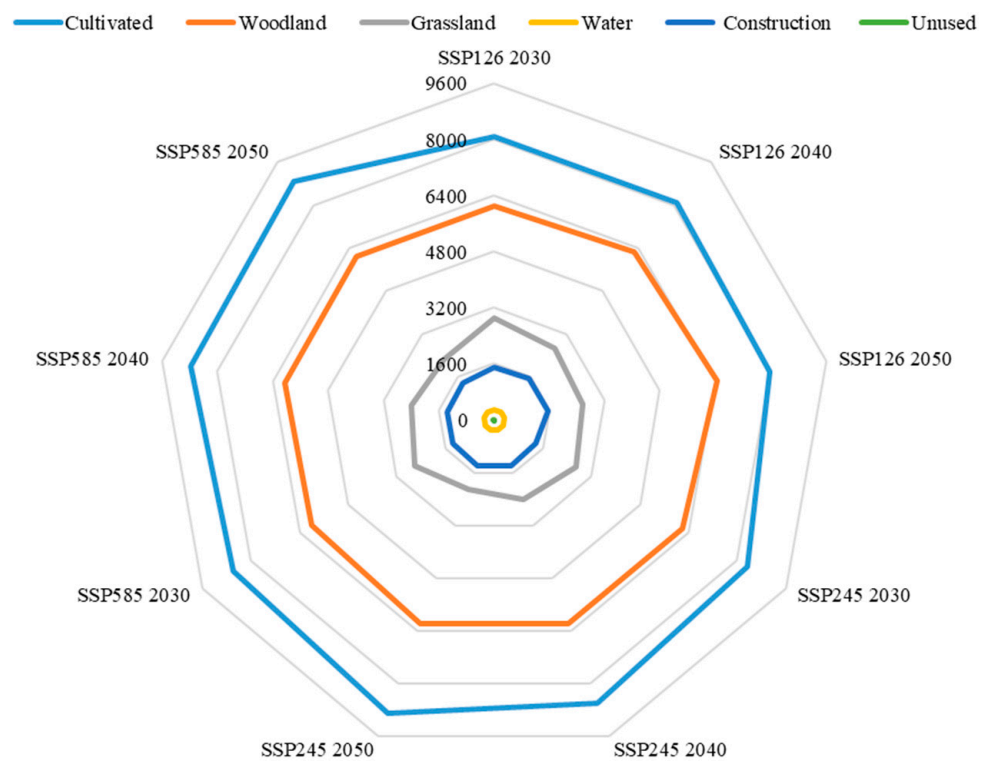


Figure 5. Overview of land-use types under different scenarios for the future period.

3.3. Changes in Carbon Storage in Historical and Future Scenarios Based on the InVEST Model

From 2000 to 2020, the overall carbon storage in the region showed a downward trend. The decrease in carbon storage from 2000 to 2010 was 399.0891×10^4 t, and from 2010 to 2020, the carbon storage decreased by 208.8340×10^4 t, with a total decrease of 607.9230×10^4 t over the past two decades. The intensity of change in the regional carbon stock coincided with the intensity of change in the built-up land, which shows that the change in land-use type affected the regional carbon stock. Limiting the transfer of land with a high carbon storage capacity and stabilizing or increasing the area of land types with a high carbon storage capacity is of great significance for the benign development of regional carbon storage capacity.

In this paper, the carbon storage values of the Yiluo River Basin were assigned to grids, and then ArcGIS was used to classify the carbon storage levels, resulting in Figure 6. From the perspective of spatial distribution, the overall distribution of carbon storage in the watershed shows a high level in the central and western regions and a low level in the eastern region. The distribution of carbon storage corresponds to the landforms of mountainous areas upstream of the watershed and hills and plains downstream. Low carbon density areas are mainly distributed near the main urban area of Luoyang City. This area is the economic center of the Yiluo River Basin, with a high population density and rapid urban development. The construction land area ratio is significant, and there is a trend of continued expansion. This phenomenon leads to land types with low carbon storage capacities constantly encroaching on land with a high carbon storage capacity, mainly around existing building areas. The areas with high carbon storage in the basin are mainly concentrated in the central and western parts of the Yiluo River Basin, with high vegetation coverage and primeval forests (Table 5).

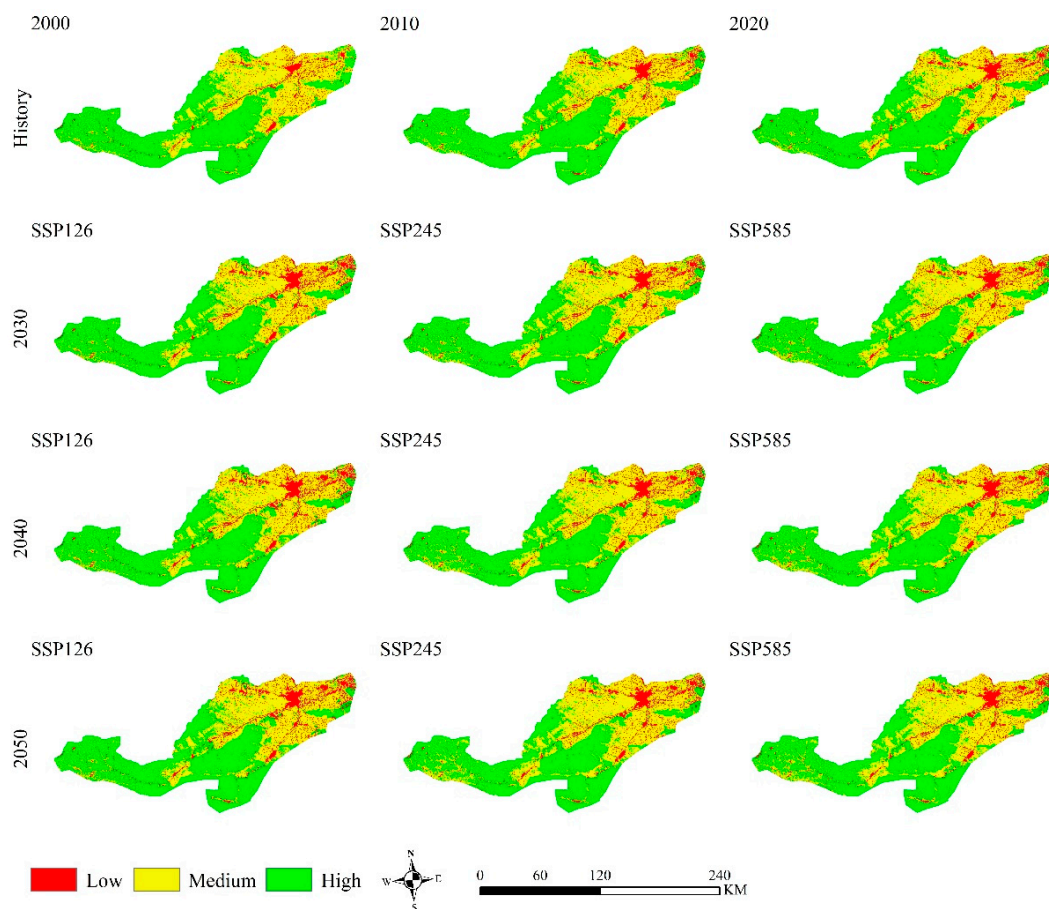


Figure 6. Distribution of carbon storage in the Yiluo River Basin in the historical and future periods.

Table 5. Carbon storage in the study area in different periods and scenarios (10^4 t).

	2000	2010	2020	2030	2040	2050
Reality	37,075.9030	36,676.8140	36,467.9800	—	—	—
SSP126	—	—	—	36,240.2765	36,227.6534	36,418.2218
SSP245	—	—	—	36,411.4745	36,327.9075	36,249.1117
SSP585	—	—	—	36,245.9717	36,204.1592	36,190.8492

Under the influence of future climate change, carbon storage in the study area under the three scenarios will decrease to different degrees compared with 2020. In the period from 2020 to 2050, the SSP126 scenario exhibits the least reduction in regional carbon storage, and in 2050, the regional carbon storage will be $36,418.2218 \times 10^4$ t, with a total reduction of 49.7582×10^4 t. In the SSP245 scenario, the regional carbon storage decreases the second most, and the carbon storage in 2050 will be $36,249.1117 \times 10^4$ t, with a total decrease of 218.8683×10^4 t. Under the SSP585 scenario, the regional carbon stock decreases the most, with a total decrease of 277.1308×10^4 t in 30 years, and the regional carbon stock in 2050 will be $36,190.8492 \times 10^4$ t (Table 5).

Figure 7 shows the spatiotemporal changes in carbon storage under multiple scenarios based on the carbon storage in the study area in 2020. The number of patches indicating an increase in carbon storage under the SSP126 scenario is much larger than that of the patches indicating increases in carbon storage under the SSP245 and SSP585 scenarios in the same period. Under the SSP126 scenario, the areas exhibiting carbon storage decreases in 2050 are mainly distributed downstream of the basin, around the main urban area of Luoyang city, and within the boundary of Zhengzhou. The main reason is that under urban development, land types with low carbon storage capacities continue to erode areas

with high carbon storage capacities. The areas with increased carbon storage are mainly distributed in the upper reaches of the basin, where the landform is mostly mountainous and there are more forest lands. Furthermore, due to topography and other reasons, other land areas have the conditions for conversion to forest lands, and the forest area has a trend of expansion, which will increase the regional carbon storage. In the SSP245 scenario, the patches indicating a reduction in carbon storage are much larger than those in the SSP126 scenario, and the distribution is scattered throughout the basin. The patches of increased carbon storage in this scenario mainly exist in the middle and upper reaches of the basin. In the SSP585 scenario, the patches representing an increase in carbon storage are the least among the three and are far smaller than those representing a decrease in carbon storage in the region, and the distribution is similar to that in the SSP245 scenario.

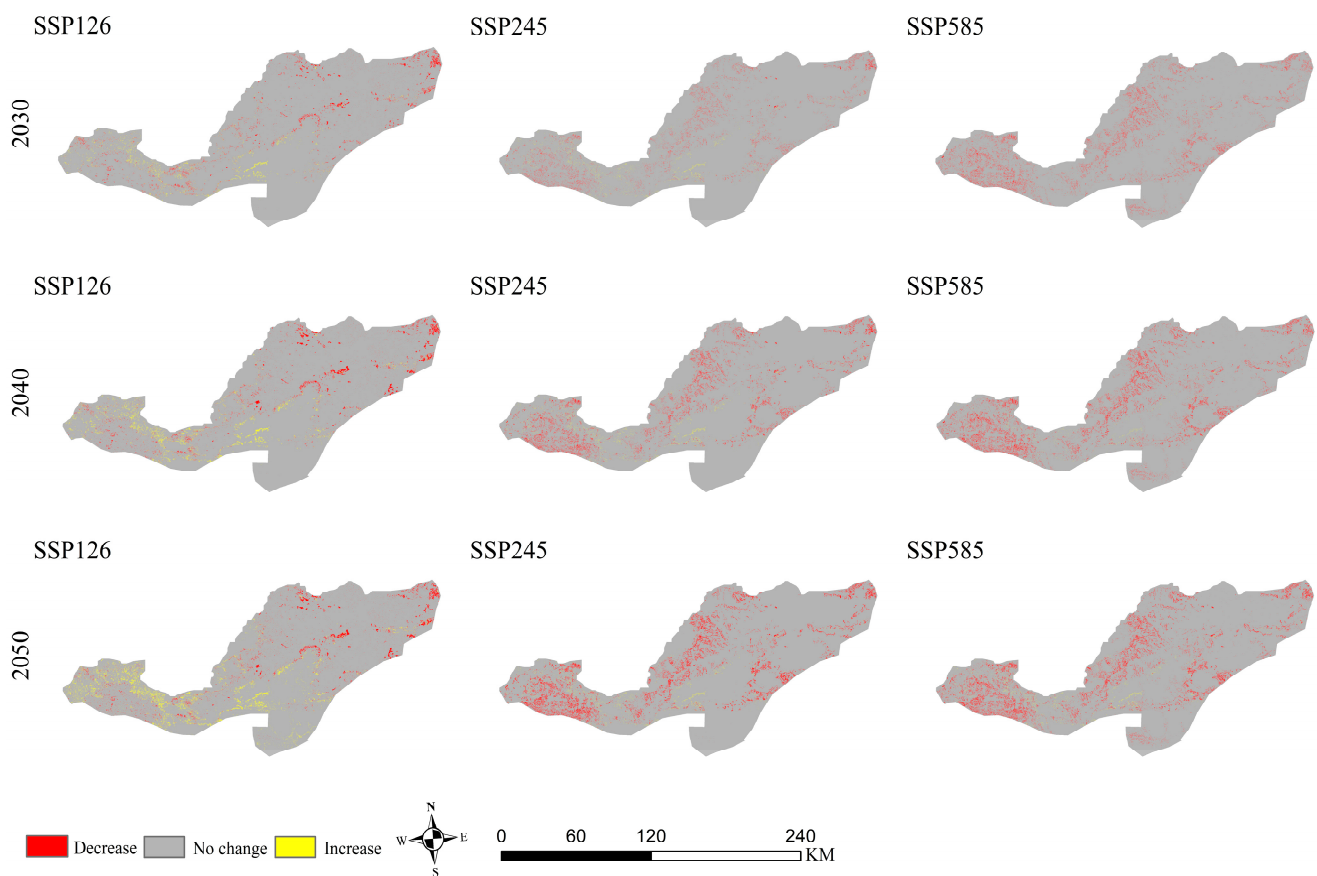


Figure 7. Changes in carbon storage in Yiluo River Basin in the future compared with 2020 under different scenarios.

4. Discussion

With the economic development of the study area, the change in land types with high carbon density values to land types with low carbon density values is the main reason for the decrease in regional carbon storage. In order to improve regional carbon storage, the conversion of cultivated land, forest land, and grassland into other land types should be controlled reasonably, and the area of land types with strong carbon storage capacities such as forest land should be appropriately increased. The future change trend of carbon storage in this paper is approximately similar to those in the studies by Yang [27] and Fan [39], and the distribution of carbon storage is similar to that in Yang's study [27]. In Yang's study, two scenarios were set up: an ecological protection scenario and a natural change scenario. In Fan's study, three scenarios were set up: business as usual, ecological conservation, and urban development scenarios. In this paper, three scenarios, SSP126, SSP245, and SSP585, were selected for research according to different paths provided by CMIP6. The land-use

demand data of the study area in different periods in the future were also derived from CMIP6 rather than being predicted by the Markov chain.

In this paper, the average annual temperature and average annual precipitation in the Yellow River Basin and Yiluo River Basin were substituted into the carbon density correction formula, and then the K_B and K_S correction coefficients were obtained, respectively. The carbon density value of the Yellow River Basin was corrected with the correction coefficient, and the required carbon density value was obtained, which was similar to that in the study by Bian [40]. The carbon density will change due to environmental changes, human activities, and other factors. This study did not continuously track and record the carbon density values in the watershed, and there may be some differences between the carbon density used and the actual carbon density, leading to slight differences in carbon storage compared with the actual situation. This study was based on three different scenarios and the PLUS model to predict the land-use types at three time nodes in 2030, 2040, and 2050, respectively. Since the time intervals are all of ten years, this paper selected a decade closer to the future (from 2010 to 2020) for the simulation. Taking 2010 as the base period, the land-use type in 2020 was predicted, and the land-use types in 2030, 2040, and 2050 were predicted after passing the test. Luoyang City has carried out a series of ecological protection actions in the new era, resulting in changes in the intensity of land-use type changes from 2010 to 2020 compared with that from 2000 to 2010. If the year 2000 is used as the base period to simulate 2010 and the future land-use types are predicted based on this, will the transformation between land-use types be greater in the future? Based on this, the InVEST model was used to calculate the total carbon storage in the Yiluo River Basin under three scenarios. The magnitude of the change in total carbon stocks and whether and how the difference between different scenarios will change remain to be discussed.

5. Conclusions

Coupling the PLUS model and the InVEST model, on the basis of clarifying the land-use changes from 2010 to 2020, combined with three different scenarios provided by CMIP6, the land use and carbon storage in the study area in 2030, 2040, and 2050 were simulated and predicted, and the impact of land-use changes on the regional carbon storage were pointed out. The main conclusions are as follows:

- (1) Land-use changes led to an increase in or loss of carbon storage. From 2000 to 2020, the areas of forest land and construction land in the Yiluo River Basin increased to varying degrees, while the areas of cultivated land, water area, grassland, and unused land decreased. The conversion of cultivated land to construction land was the main transfer type, which was also an important reason for the decrease in regional carbon storage.
- (2) Under the three scenarios, the proportion of cultivated land area in the SSP126 scenario was the smallest, while the proportions of woodland and grassland areas in this scenario were the largest. All three scenarios had some protection of forest land area and none of them showed a significant reduction.
- (3) From 2020 to 2050, the carbon storage in the study area under the three scenarios of SSP126, SSP245, and SSP585 all show varying degrees of decline, decreasing to $36,418.2218 \times 10^4$ t, $36,249.1117 \times 10^4$ t, and $36,190.8492 \times 10^4$ t, respectively. Forest land, grassland, and cultivated land have strong carbon storage capacities, and limiting the conversion of land with a high carbon storage capacity to land with a low carbon storage capacity is conducive to the benign development of regional carbon storage capacity.

Author Contributions: Conceptualization, G.L.; methodology, L.L.; software, J.Z. and L.L.; formal analysis, M.J.; data curation, L.L., M.L. and H.G.; writing—original draft, L.L.; writing—review and editing, L.L., G.J., Q.L. and M.L.; project administration, G.L., G.J. and Q.L.; funding acquisition, G.L., G.J. and Q.L. All authors have read and agreed to the published version of the manuscript.

Funding: This research was funded by the National Key R&D Program of China (2021YFD1700900), the Special Fund for Top Talents of Henan Agricultural University (30501031), the National Development and Reform Commission Energy Bureau Project ([2017]20-24), the Henan Agricultural University Graduate Education Reform Project (NDYJSJG2021-15), and the Study on High-Quality Development Path of Grain Production in Henan Province (SKL-2023-2727).

Data Availability Statement: The data presented in this study are available on request from the corresponding author.

Conflicts of Interest: The authors declare no conflict of interest.

References

- Zou, S.; Zhang, T. CO₂ Emissions, Energy Consumption, and Economic Growth Nexus: Evidence from 30 Provinces in China. *Math. Probl. Eng.* **2020**, *2020*, 8842770. [[CrossRef](#)]
- Siqin, Z.; Niu, D.; Li, M.; Zhen, H.; Yang, X. Carbon dioxide emissions, urbanization level, and industrial structure: Empirical evidence from North China. *Environ. Sci. Pollut. Res.* **2022**, *29*, 34528–34545. [[CrossRef](#)]
- Giersch, J.J.; Hotaling, S.; Kovach, R.P.; Jones, L.A.; Muhlfeld, C.C. Climate-induced glacier and snow loss imperils alpine stream insects. *Glob. Chang. Biol.* **2017**, *23*, 2577–2589. [[CrossRef](#)]
- Li, L.; Fu, W.; Luo, M. Spatial and Temporal Variation and Prediction of Ecosystem Carbon Stocks in Yunnan Province Based on Land Use Change. *Int. J. Environ. Res. Public Health* **2022**, *19*, 16059. [[CrossRef](#)]
- Bo, C.; Chong, X.; Yin, W.; Zhi, L.; Ma, S.; Zhi, S. Spatiotemporal carbon emissions across the spectrum of Chinese cities: Insights from socioeconomic characteristics and ecological capacity. *J. Environ. Manag.* **2022**, *306*, 114510. [[CrossRef](#)]
- Tao, Y.; Li, F.; Wang, R.; Zhao, D. Effects of land use and cover change on terrestrial carbon stocks in urbanized areas: A study from Changzhou, China. *J. Clean. Prod.* **2015**, *103*, 651–657. [[CrossRef](#)]
- Du, S.; Zhou, Z.; Huang, D.; Zhang, F.; Deng, F.; Yang, Y. The Response of Carbon Stocks to Land Use/Cover Change and a Vulnerability Multi-Scenario Analysis of the Karst Region in Southern China Based on PLUS-InVEST. *Forests* **2023**, *14*, 2307. [[CrossRef](#)]
- Sun, F.H.; Fang, F.M.; Hong, W.L.; Luo, H.; Yu, J.; Fang, L.; Miao, Y.Q. Evolution Analysis and Prediction of Carbon Storage in Anhui Province Based on PLUS and InVEST Model. *J. Soil Water Conserv.* **2023**, *37*, 151–158. (In Chinese) [[CrossRef](#)]
- Zheng, H.; Zheng, H. Assessment and prediction of carbon storage based on land use/land cover dynamics in the coastal area of Shandong Province. *Ecol. Indic.* **2023**, *153*, 110474. [[CrossRef](#)]
- Piyathilake, I.D.U.H.; Udayakumara, E.P.N.; Ranaweera, L.V.; Gunatilake, S.K. Modeling predictive assessment of carbon storage using InVEST model in Uva province, Sri Lanka. *Model. Earth Syst. Environ.* **2022**, *8*, 2213–2223. [[CrossRef](#)]
- Tadese, S.; Soromessa, T.; Aneseye, A.B.; Gebeyehu, G.; Noszczyk, T.; Kindu, M. The impact of land cover change on the carbon stock of moist afro-montane forests in the Majang Forest Biosphere Reserve. *Carbon Balance Manag.* **2023**, *18*, 24. [[CrossRef](#)] [[PubMed](#)]
- Rajbanshi, J.; Das, S. Changes in carbon stocks and its economic valuation under a changing land use pattern—A multitemporal study in Konar catchment, India. *Land Degrad. Dev.* **2021**, *32*, 3573–3587. [[CrossRef](#)]
- Xie, T.Q.; Li, L.; Chen, X.; Bai, L.; Xia, L.; Wang, C.; Li, T. Estimation and prediction of carbon storage based on land use in the Huaihai Economic Zone. *J. China Agric. Univ.* **2021**, *26*, 131–142. (In Chinese)
- Wang, C.Y.; Gao, X.H.; Guo, L.; Bai, L.F.; Xia, L.L.; Wang, C.B.; Li, T.Z. Land Use Change and Its Impact on Carbon Storage in Northwest China Based on FLUS-Invest: A Case Study of Hu-Bao-Er-Yu Urban Agglomeration. *Ecol. Environ. Sci.* **2022**, *31*, 1667–1679. (In Chinese) [[CrossRef](#)]
- Qing, M.; Zhao, J.; Feng, C.; Huang, Z.H.; Wen, Y.Y.; Zhang, W.J. Response of ecosystem carbon storage service to land-use change in Shiyang River Basin from 1980 to 2030. *Acta Ecol. Sin.* **2022**, *42*, 9525–9536. (In Chinese)
- Wang, R.; Zhao, J.; Chen, G.; Lin, Y.; Yang, A.; Cheng, J. Coupling PLUS-InVEST Model for Ecosystem Service Research in Yunnan Province, China. *Sustainability* **2023**, *15*, 271. [[CrossRef](#)]
- Liang, X.; Guan, Q.; Clarke, K.C.; Liu, S.; Wang, B.; Yao, Y. Understanding the drivers of sustainable land expansion using a patch-generating land use simulation (PLUS) model: A case study in Wuhan, China. *Comput. Environ. Urban Syst.* **2021**, *85*, 101569. [[CrossRef](#)]
- Li, P.; Chen, J.; Li, Y.; Wu, W. Using the InVEST-PLUS Model to Predict and Analyze the Pattern of Ecosystem Carbon storage in Liaoning Province, China. *Remote Sens.* **2023**, *15*, 4050. [[CrossRef](#)]
- Yue, S.; Ji, G.; Chen, W.; Huang, J.; Guo, Y.; Cheng, M. Spatial and Temporal Variability Characteristics of Future Carbon Stocks in Anhui Province under Different SSP Scenarios Based on PLUS and InVEST Models. *Land* **2023**, *12*, 1668. [[CrossRef](#)]

20. Huang, Y.; Xie, F.; Song, Z.; Zhu, S. Evolution and Multi-Scenario Prediction of Land Use and Carbon Storage in Jiangxi Province. *Forests* **2023**, *14*, 1933. [[CrossRef](#)]
21. Wu, F.; Wang, Z. Assessing the impact of urban land expansion on ecosystem carbon storage: A case study of the Changzhutan metropolitan area, China. *Ecol. Indic.* **2023**, *154*, 110688. [[CrossRef](#)]
22. Sun, X.-X.; Wang, S.-G.; Xue, J.-H.; Dong, L.-N. Assessment and simulation of ecosystem carbon storage in rapidly urbanizing areas based on land use cover: A case study of the southern Jiangsu urban agglomeration, China. *Front. Ecol. Evol.* **2023**, *11*, 1197548. [[CrossRef](#)]
23. Wang, Y.; Liang, D.; Wang, J.; Zhang, Y.; Chen, F.; Ma, X. An analysis of regional carbon stock response under land use structure change and multi-scenario prediction, a case study of Hefei, China. *Ecol. Indic.* **2023**, *151*, 110293. [[CrossRef](#)]
24. Chen, L.; Ma, Y. Exploring the Spatial and Temporal Changes of Carbon Storage in Different Development Scenarios in Foshan, China. *Forests* **2022**, *13*, 2177. [[CrossRef](#)]
25. Wang, X.; Wang, C.Y.; Lv, F.N.; Chen, S.L.; Yu, Z.R. Temporal and spatial carbon storage change and carbon sink improvement strategy of district and county level based on PLUS-InVEST model: Taking Yangting District as an example. *Chin. J. Appl. Ecol.* **2023**, *in press*. (In Chinese) [[CrossRef](#)]
26. Huang, Y.; Li, X.P.; Zhao, N.; Niu, X.L.; Yin, D.X.; Qin, D. Analysis on Characteristics of Temporal and Spatial Changes of Land Use in the Yiluo River Basin. *Spectrosc. Spectr. Anal.* **2022**, *42*, 3180–3186. (In Chinese)
27. Yang, J.; Xie, B.P.; Zhang, D.G. Spatio-temporal evolution of carbon stocks in the Yellow River Basin based on InVEST and CA-Markov models. *Chin. J. Eco-Agric.* **2021**, *29*, 1018–1029. (In Chinese) [[CrossRef](#)]
28. Ling, M.; Yang, Y.; Xu, C.; Yu, L.; Xia, Q.; Guo, X. Temporal and Spatial Variation Characteristics of Actual Evapotranspiration in the Yiluo River Basin Based on the Priestley–Taylor Jet Propulsion Laboratory Model. *Appl. Sci.* **2022**, *12*, 9784. [[CrossRef](#)]
29. Li, Q.; Pu, Y.; Gao, W. Spatial correlation analysis and prediction of carbon stock of “Production-living-ecological spaces” in the three northeastern provinces, China. *Heliyon* **2023**, *9*, e18923. [[CrossRef](#)]
30. Luo, S.Q.; Hu, X.M.; Sun, Y.; Yan, C.; Zhang, X. Multi-scenario land use change and its impact on carbon storage based on coupled Plus-Invest model. *Chin. J. Eco-Agric.* **2023**, *31*, 300–314. (In Chinese) [[CrossRef](#)]
31. Zhu, Z.Q.; Ma, X.S.; Hu, H. Spatio-temporal Evolution and Prediction of Ecosystem Carbon Stocks in Guangzhou City by Coupling FLUS-InVEST Models. *Bull. Soil Water Conserv.* **2021**, *41*, 222–229+239. (In Chinese) [[CrossRef](#)]
32. Zhu, J.; Hu, X.; Xu, W.; Shi, J.; Huang, Y.; Yan, B. Regional Carbon Stock Response to Land Use Structure Change and Multi-Scenario Prediction: A Case Study of Hunan Province, China. *Sustainability* **2023**, *15*, 12178. [[CrossRef](#)]
33. Hou, J.; Qin, T.; Yan, D.; Feng, J.; Liu, S.; Zhang, X.; Li, C. Evaluation of water-land resources regulation potential in the Yiluo River Basin, China. *Ecol. Indic.* **2023**, *153*, 110410. [[CrossRef](#)]
34. Alam, S.; Starr, M.; Clark, B. Tree biomass and soil organic carbon densities across the Sudanese woodland savannah: A regional carbon sequestration study. *J. Arid. Environ.* **2013**, *89*, 67–76. [[CrossRef](#)]
35. Giardina, C.; Ryan, M. Evidence that decomposition rates of organic carbon in mineral soil do not vary with temperature. *Nature* **2000**, *404*, 858–861. [[CrossRef](#)]
36. Chen, G.S.; Yang, Y.S.; Liu, L.Z.; Li, X.B.; Zhao, Y.C.; Yuan, Y.D. Research Review on Total Belowground Carbon Allocation in Forest Ecosystems. *J. Subtrop. Resour. Environ.* **2007**, *2*, 34–42. (In Chinese) [[CrossRef](#)]
37. Hurtt, G.C.; Chini, L.P.; Sahajpal, R.; Frolking, S.; Boudirsky, B.L.; Calvin, K.V.; Doelman, J.C.; Fisk, J.P.; Fujimori, S.; Klein Goldewijk, K.; et al. Harmonization of global land use change and management for the period 850–2100 (LUH2) for CMIP6. *Geosci. Model Dev.* **2020**, *13*, 11. [[CrossRef](#)]
38. O’Neill, B.C.; Tebaldi, C.; van Vuuren, D.P.; Eyring, V.; Friedlingstein, P.; Hurtt, G.; Knutti, R.; Kriegler, E.; Lamarque, J.-F.; Lowe, J.; et al. The Scenario Model Intercomparison Project (ScenarioMIP) for CMIP6. *Geosci. Model Dev.* **2016**, *9*, 3461–3482. [[CrossRef](#)]
39. Fan, L.; Cai, T.; Wen, Q.; Han, J.; Wang, S.; Wang, J.; Yin, C. Scenario simulation of land use change and carbon storage response in Henan Province, China: 1990–2050. *Ecol. Indic.* **2023**, *154*, 110660. [[CrossRef](#)]
40. Bian, R.; Zhao, A.Z.; Liu, X.F.; Xu, R.H.; Li, Z.Y. Impact of Land Use Change on Carbon Storage in Urban Agglomerations in the Guanzhong Plain. *Environ. Sci.* **2023**, *in press*. (In Chinese) [[CrossRef](#)]

Disclaimer/Publisher’s Note: The statements, opinions and data contained in all publications are solely those of the individual author(s) and contributor(s) and not of MDPI and/or the editor(s). MDPI and/or the editor(s) disclaim responsibility for any injury to people or property resulting from any ideas, methods, instructions or products referred to in the content.